Exploring residue component contributions to dynamical network models of allostery

Adam T. VanWart [1], John Eargle [2], Zaida Luthey-Schulten [2], and Rommie E. Amaro [1*]

1 Department of Chemistry and Biochemistry, University of California, San Diego, La Jolla, CA 92093
2 Department of Chemistry, University of Illinois at Urbana-Champaign, Urbana, IL 61801

Supplemental Information

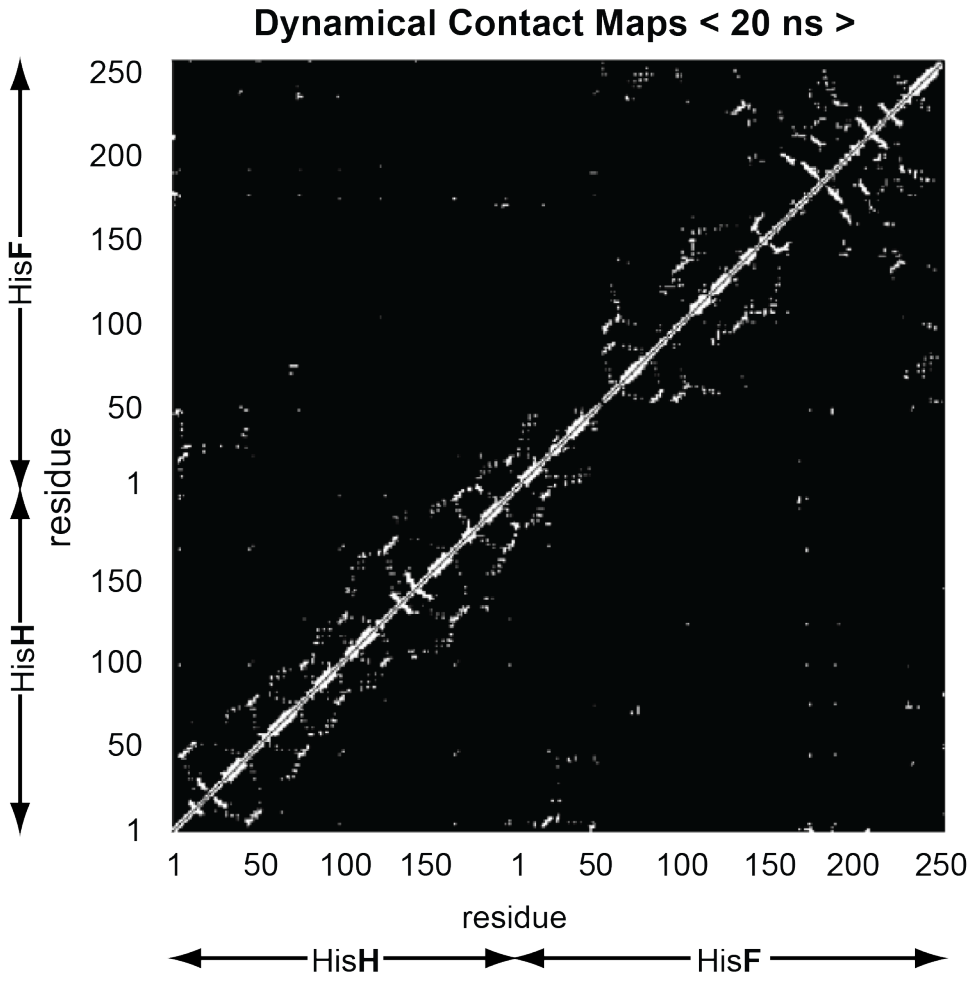

SI figure 1
The above contact map was generated over the 20 ns of production molecular dynamics. If residues were within 4.5 Å of another residue for 75% of the 40,000 frame (20 ns) trajectory, the correlation value in the correlation matrix was kept (white); conversely the correlation value would be zero (black). All calculations used this matrix when deriving optimal paths for the holo-state HisH-HisF including the optimal pathways in the convergence tables. An analogous contact map was made for the apo-state.

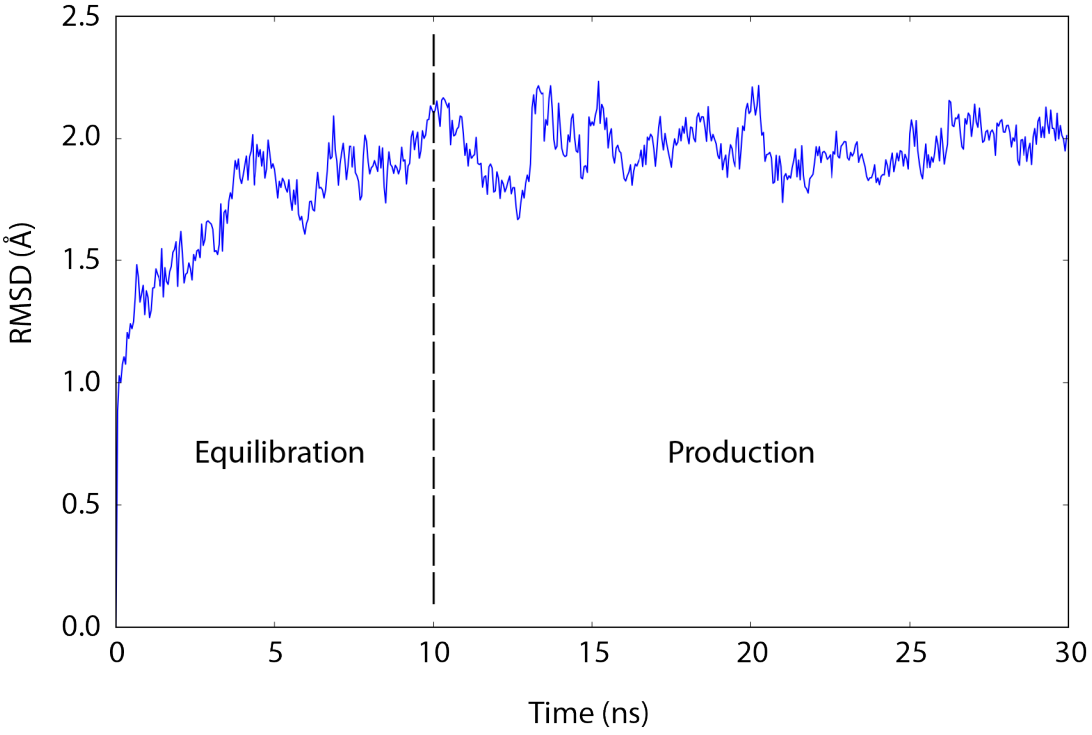

SI figure 2
The figure above shows the RMSD for our 30 ns molecular dynamics simulation of hisH-hisF with PRFAR bound. Frames were aligned to the average structure and the RMSD was calculated relative to the first frame. The first 10 ns of dynamics were discarded and were mainly used as a cautionary measure for assurance of equilibrium since the crystal structure (1gpw chains C D) did not have PRFAR resolved. The remaining 20 ns of production dynamics were used as data for optimal pathways as well as community analysis.

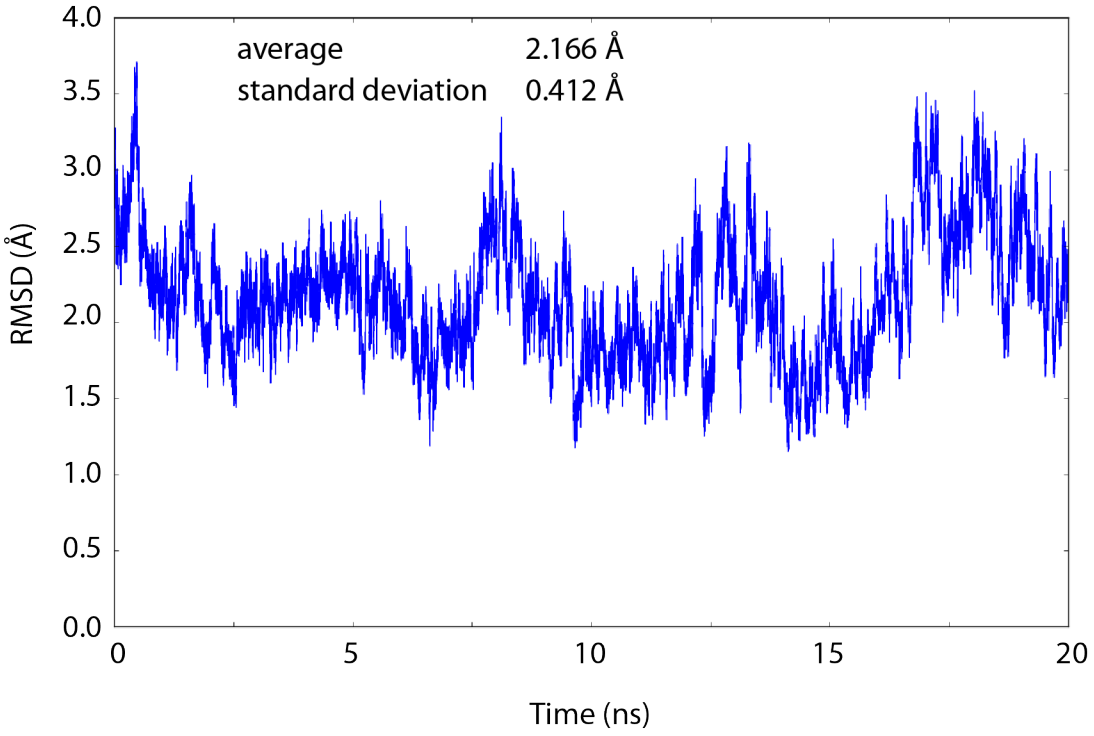

SI figure 3
Depicted above is the holo-state root mean squared deviation (RMSD) for all atoms in residues HisF:Lys19 thru HisF:Glu34 and residue HisF:Ile52. This RMSD is taken relative to the average structure of the entire protein and approximates the RMSF assuming equilibrium conditions. The residues were chosen since they comprise a large part of the loop structure at the C-terminal end of the $(\beta/\alpha)_8$ barrel and because they form the intersection between the members of the black community in the apo-state and the members of the black community in the holo-state (figure 7). The holo-state RMSD has a higher fluctuation and standard deviation than that of the apo-state suggesting a looser conformation and greater fluctuation for the loop. Furthermore, the ImGP moiety is a member of the holo-state black community and is seen to directly impact the black community shift from the apo-state to the holo-state.

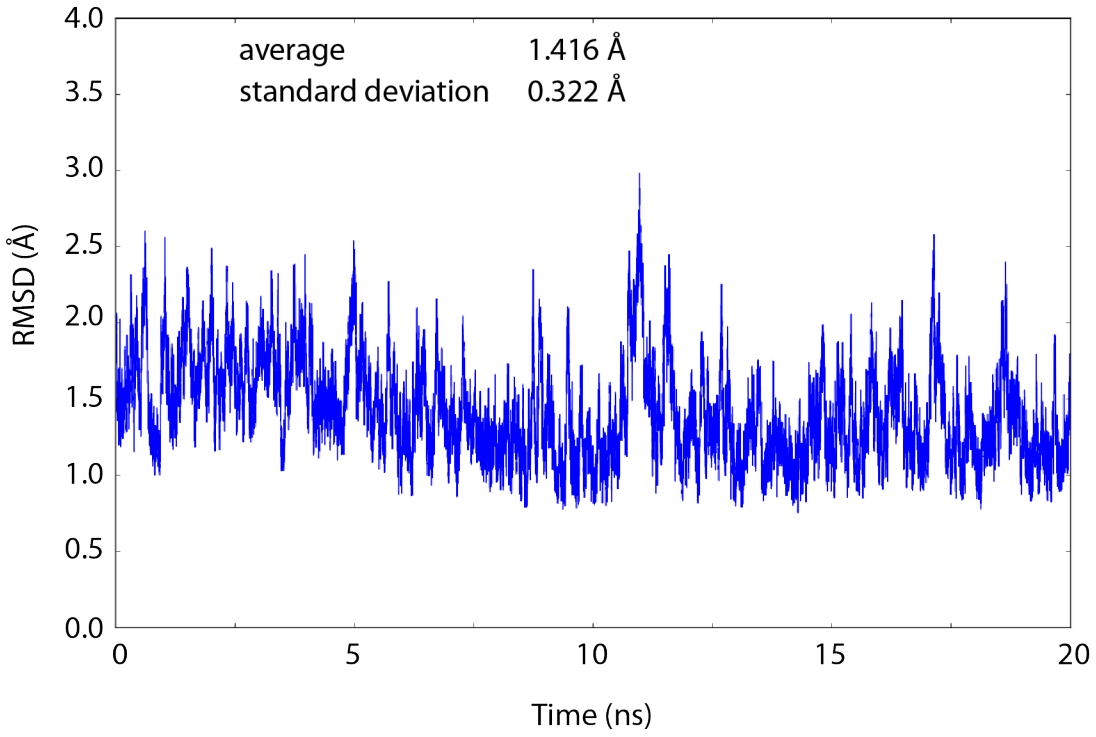

SI figure 4
Depicted above is the apo-state root mean squared deviation (RMSD) for residues HisF:Lys19 thru HisF:Glu34 and residue HisF:Ile52. This RMSD is also taken relative to the average structure of the entire protein and approximates the RMSF assuming equilibrium conditions. The residues were chosen for the same reasons explained in SI figure 3. The apo-state RMSD has a smaller fluctuation and standard deviation than that of the holo-state suggesting a tighter conformation of the loop at the C-terminal end of the $(\beta/\alpha)_8$ barrel.

ImGP-(HisH:Glu180)

			HisF													HisH	
Node Method	time (ns)	ImGP	Leu	Phe	Val	Leu	Ile	Gly	Val	Thr	Phe	Pro	Ile	Asp	Lys	Asp	Lys	Glu
Side-chain	< 5 >	ImGP	50		48	47							75	74				180
c.o.m.	< 10 >	ImGP	50	49			73							74				180
	< 15 >	ImGP	50		48					78					99	98	181	180
	< 20 >	ImGP	50		48					78					99	98	181	180
Residue	< 5 >	ImGP	50					80	79						99	98	181	180
c.o.m.	< 10 >	ImGP	50					80	79						99	98	181	180
	< 15 >	ImGP	50					80	79						99	98	181	180
	< 20 >	ImGP	50					80	79						99	98	181	180
alpha-carbon	< 5 >	ImGP	50	49	48	47						76					181	180
	< 10 >	ImGP	50	49						78	77	76					181	180
	< 15 >	ImGP	50	49						78	77	76					181	180
	< 20 >	ImGP	50	49							77	76					181	180
Backbone	< 5 >	ImGP	50	49						78	77	76					181	180
c.o.m.	< 10 >	ImGP	50	49						78	77	76					181	180
	< 15 >	ImGP	50	49						78	77						181	180
	< 20 >	ImGP	50	49						78	77						181	180

AICAR-(HisH:Glu180)

			HisF																							HisH	
Node Method	time (ns)	AICAR	Thr	Ala	Val	Asp	Lys	Val	Val	Asp	Pro	Val	Cys	Ala	Leu	Phe	Val	Leu	Glu	Gln	Ile	Gly	Val	Thr	Phe	Pro	Ile	Asp	Lye	Asp	Lys	Glu
Side-chain	< 5 >	AICAR											9				48	47									75	74				180
c.o.m.	< 10 >	AICAR				11			17		32	33								72								74				180
	< 15 >	AICAR											9				48							78					99	98	181	180
	< 20 >	AICAR											9				48							78					99	98	181	180
Residue	< 5 >	AICAR											9				48		46							76					181	180
c.o.m.	< 10 >	AICAR				11									50							80	79						99	98	181	180
	< 15 >	AICAR	171	128	126																								99	98	181	180
	< 20 >	AICAR	171	128	126																								99	98	181	180
alpha-carbon	< 5 >	AICAR											9				48	47								76					181	180
	< 10 >	AICAR				11									50	49								78	77	76					181	180
	< 15 >	AICAR													50	49								78	77	76					181	180
	< 20 >	AICAR													50	49									77	76					181	180
Backbone	< 5 >	AICAR											9	8					46								75	74				180
c.o.m.	< 10 >	AICAR					19	18	17	31		33								72	73							74				180
	< 15 >	AICAR													50	49								78	77						181	180
	< 20 >	AICAR													50	49								78	77						181	180

ImGP-(HisH:His178)

			HisF													HisH		
Node Method	time (ns)	ImGP	Leu	Phe	Val	Leu	Glu	Gly	Val	Thr	Phe	Pro	Ile	Arg	Lys	Tyr	Lys	His
Side-chain	< 5 >	ImGP	50		48								7	5		138		178
c.o.m.	< 10 >	ImGP	50		48		46									138		178
	< 15 >	ImGP	50		48					78					99	138		178
	< 20 >	ImGP	50		48					78					99	138		178
Residue	< 5 >	ImGP	50		48		46									138		178
c.o.m.	< 10 >	ImGP	50					80	79						99	138		178
	< 15 >	ImGP	50		48		46									138		178
	< 20 >	ImGP	50		48		46									138		178
alpha-carbon	< 5 >	ImGP	50	49	48		46									138		178
	< 10 >	ImGP	50	49	48	47	46									138		178
	< 15 >	ImGP	50	49						78	77	76				181		178
	< 20 >	ImGP	50	49							77	76				181		178
Backbone	< 5 >	ImGP	50	49	48		46									138		178
c.o.m.	< 10 >	ImGP	50	49						78	77	76				138		178
	< 15 >	ImGP	50	49						78	77	76				138		178
	< 20 >	ImGP	50	49	48	47	46									138		178

AICAR-(HisH:His178)

			HisF																	HisH		
Node Method	time (ns)	AICAR	Thr	Ala	Val	Cys	Ala	Leu	Phe	Val	Leu	Glu	Thr	Phe	Pro	Ile	Ile	Arg	Lys	Asp	Tyr	Lys	His
Side-chain	< 5 >	AICAR				9										7		5			138		178
c.o.m.	< 10 >	AICAR				9				48		46									138		178
	< 15 >	AICAR				9				48			78						99		138		178
	< 20 >	AICAR				9				48			78						99		138		178
Residue	< 5 >	AICAR				9	8									7		5			138		178
c.o.m.	< 10 >	AICAR				9				48		46									138		178
	< 15 >	AICAR	171	128	126														99	98		181	178
	< 20 >	AICAR				9	8					46									138		178
alpha-carbon	< 5 >	AICAR				9	8									7		5			138		178
	< 10 >	AICAR				9				48	47	46									138		178
	< 15 >	AICAR						50	49				78	77	76							181	178
	< 20 >	AICAR						50	49					77	76							181	178
Backbone	< 5 >	AICAR				9	8										6	5			138		178
c.o.m.	< 10 >	AICAR				9	8					46									138		178
	< 15 >	AICAR						50	49				78	77	76						138		178
	< 20 >	AICAR				9	8					46									138		178

SI table 1

The tables above show combinations of pathways between PRFAR moieties (AICAR and ImGP) and residues in the catalytic triad (Glu180 and Hsd178). The third residue in the catalytic triad, Cys84, gave degenerate data, Cys84 coupled to Hsd178 every time, and is

not shown. Optimal pathways showed consistency over the average structures for 5, 10, 15 and 20 ns. The optimal pathway for source ImGP to sink Glu180 is assumed to have completely converged.

ImGP-(HisH:Glu180)

			HisF								HisH		
HisH-HisF	time (ns)	ImGP	Leu	Phe	Gly	Val	Phe	Pro	Lys	Asp	Lys	Glu	distance
Holo-residue c.o.m.	< 20 >	ImGP	50		80	79			99	98	181	180	287
Apo-residue c.o.m.	< 20 >	none	50	49			77	76			181	180	298

AICAR-(HisH:Glu180)

			HisF							HisH		
HisH-HisF	time (ns)	AICAR	Thr	Ile	Val	Ala	Val	Lys	Asp	Lys	Glu	distance
Holo-residue c.o.m.	< 20 >	AICAR	171			128	126	99	98	181	180	295
Apo-residue c.o.m.	< 20 >	none	171	129	127		126	99	98	181	180	362

ImGP-(HisH:His178)

			HisF							HisH		
HisH-HisF	time (ns)	ImGP	Leu	Phe	Val	Glu	Phe	Pro	Tyr	His		distance
Holo-residue c.o.m.	< 20 >	ImGP	50		48	46			138	178		303
Apo-residue c.o.m.	< 20 >	none	50	49			77	76	138	178		314

AICAR-(HisH:His178)

			HisF					HisH		
HisH-HisF	time (ns)	AICAR	Cys	Ala	Glu	Pro	Tyr	His		distance
Holo-residue c.o.m.	< 20 >	AICAR	9	8	46		138	178		301
Apo-residue c.o.m.	< 20 >	none	9	8	46	76	138	178		310

SI table 2

Above are the holo-state and analogous apo-state optimal pathways. The center of mass method is used for comparison across both states, and the source is omitted for the apo-state since PRFAR is not present. The distance values are calculated according to eq. 4.